

雷达观测量：反射率

The received power $P_r = \frac{c_2 Z}{r^2}$

c_2 Radar constant, $\sim 1/\lambda^2$

Z Radar reflectivity factor

- A quantity determined by the drop-size distribution of precipitation.

r distance from the target to the radar

雷达观测量：反射率

Reflectivity factor

$$Z = \int_0^{\infty} N(D) D^6 dD.$$

N : drop-size distribution

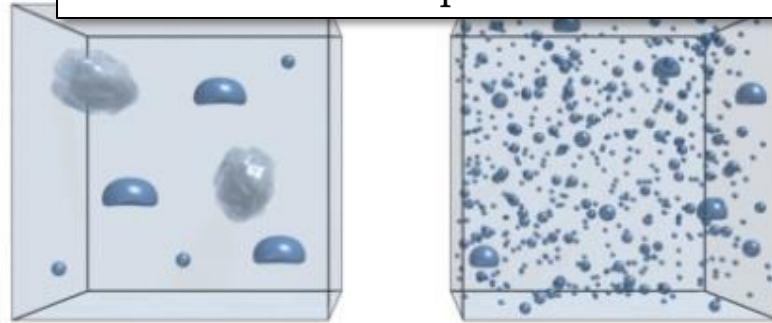
$$Z = \sum_{i=1}^n D_i^6$$

$\text{mm}^6 \text{m}^{-3}$

Rayleigh scattering theory gives the backscattering cross section of a spherical droplet of diameter D as

$$\sigma = \frac{\pi^5}{\lambda^4} |K|^2 D^6, \quad (15)$$

where K is the complex index of refraction.



Nonprecipitating cloud: 10^{-5} - 10^1

Hail: 10^7

假定 $t = 0$ 时雷达距离目标物的距离为 R_0 , 目标物朝雷达移动, 则 t 接收时刻目标物到雷达的距离为:

$$R(t) = R_0 - v_r t \quad t_r = \frac{2R(t)}{c} = \frac{2}{c}(R_0 - v_r t)$$

$$\begin{aligned} \text{相位差 } \varphi(t) &= -\omega_0 t_r = -\omega_0 \frac{2}{c}(R_0 - v_r t) \\ &= -2\pi \frac{c}{\lambda} \frac{2}{c}(R_0 - v_r t) \\ &= -2\pi \frac{2}{\lambda}(R_0 - v_r t) \end{aligned}$$

频率差 (假定 v_r 为常数)

$$f_d = \frac{1}{2\pi} \frac{d\varphi}{dt} = \frac{2v_r}{\lambda} \Rightarrow v_r = \frac{f_d \lambda}{2}$$

Radar Assumptions

Angle

1. The beam **travels** at the original inclination angle.

Attenuation

2. The targets **absorb very little** of the radar's electromagnetic **energy**.

Homogeneity

3. Target particles are **small, homogeneous** precipitation **spheres** with **diameters** much smaller than the radar's wavelength.

Phase

4. All targets are **either liquid or frozen**, but not a mixture.

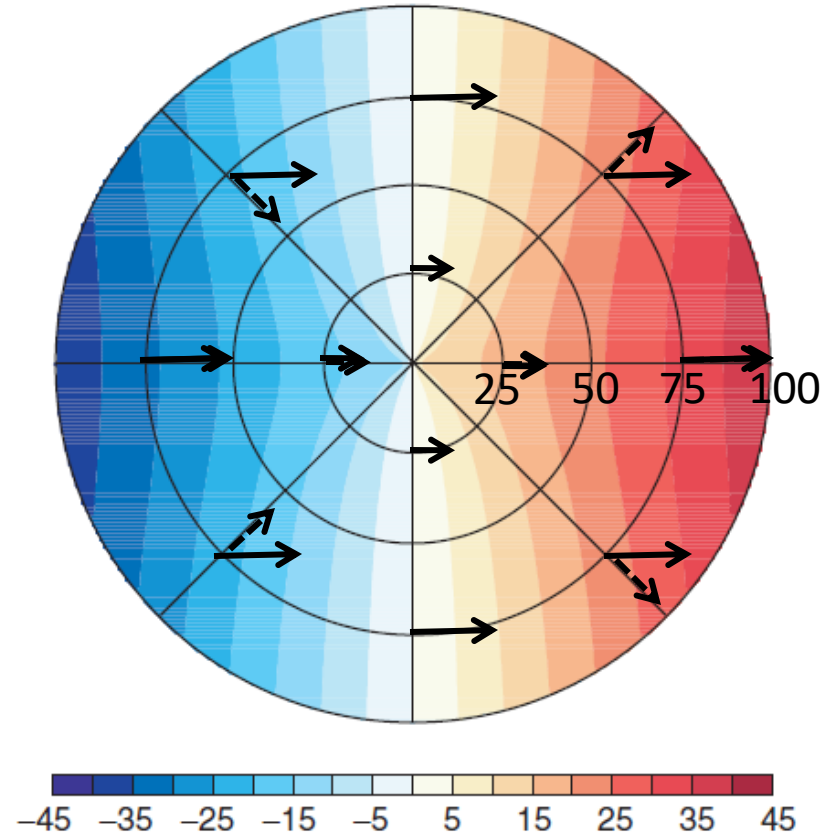
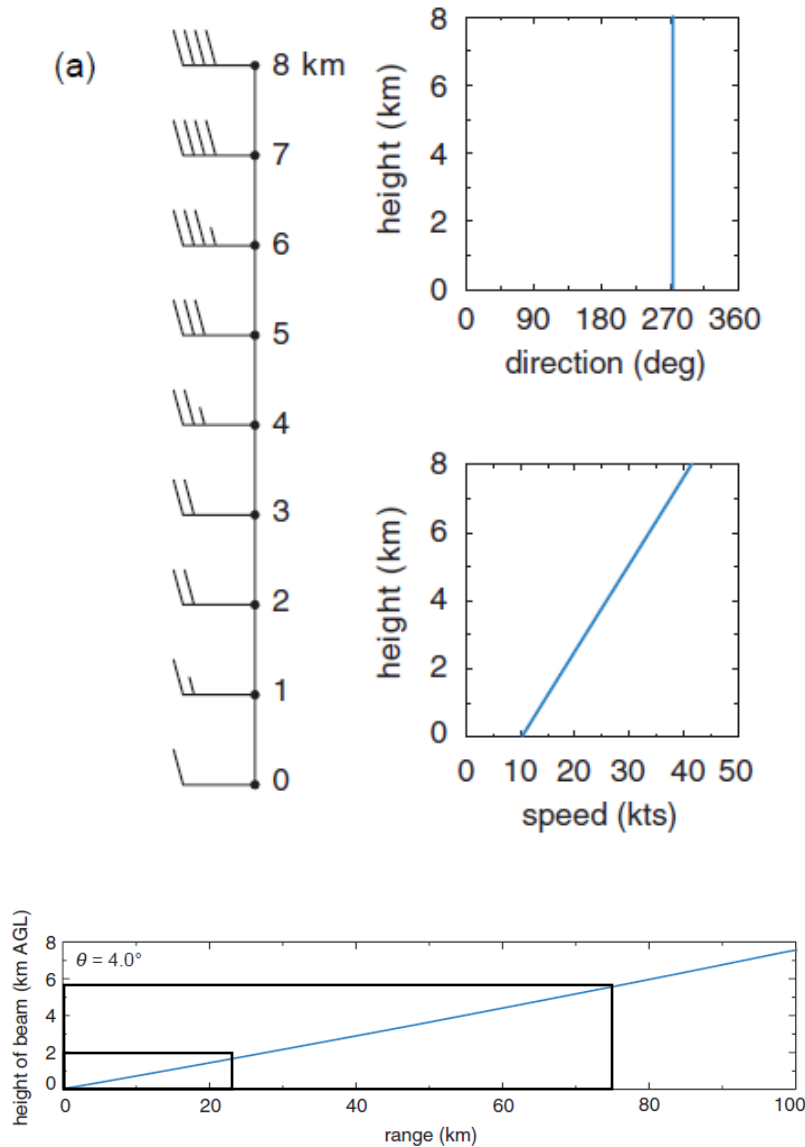
Uniformity

5. Targets are **uniformly distributed** throughout the sample volume.

上节课回顾

Westerly wind increasing in magnitude with height

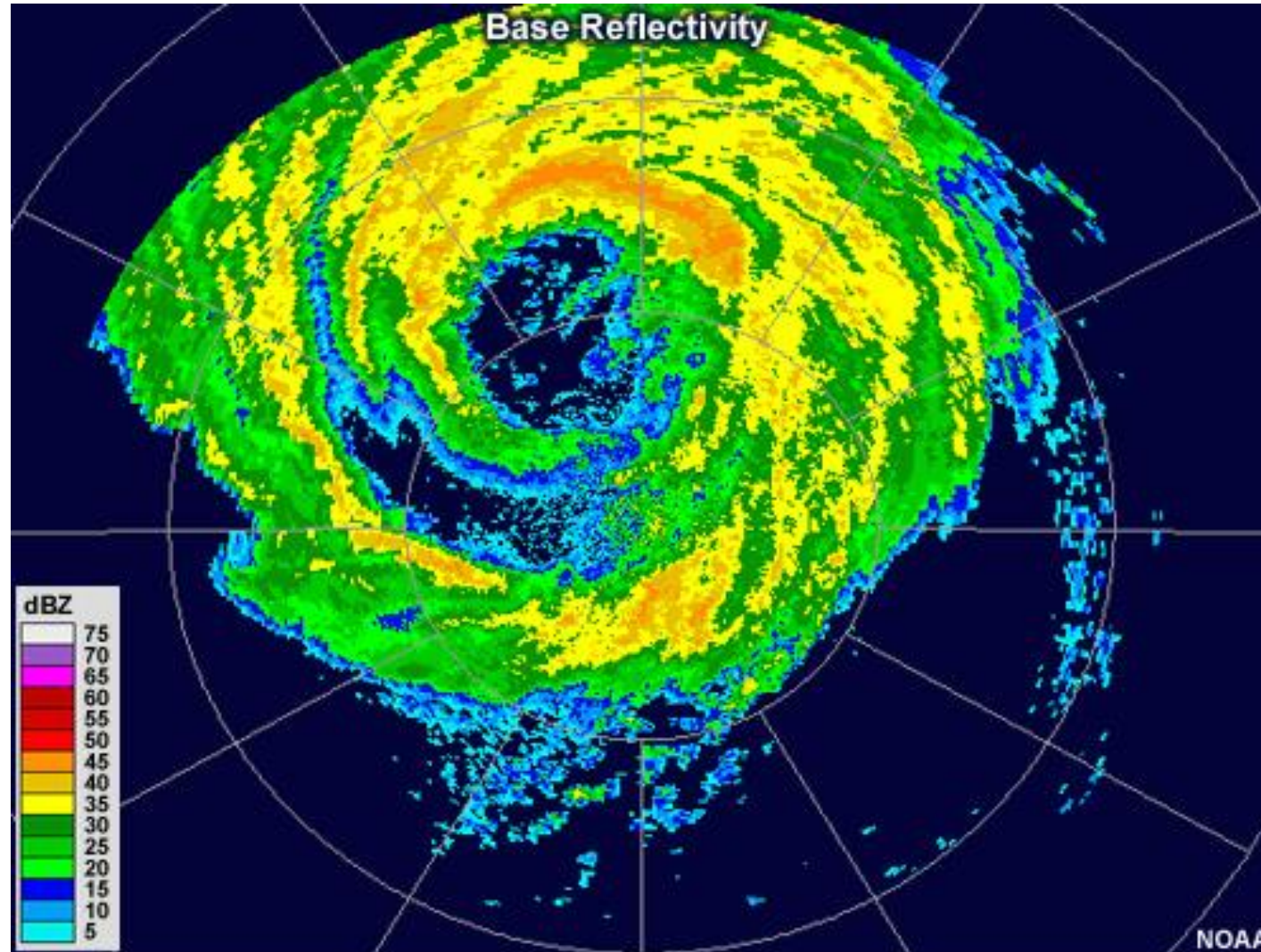
练习: 1.标风矢量, 2. 雷达测到的风 at 20 and 60 km



Cool colors
Negative (-)
TOWARD radar
along radial.

Warm colors
Positive (+)
AWAY FROM
radar along radial.

Tropical Cyclone





1.1 什么是中尺度

1.2 中尺度基本方程组

1.3 扰动气压

1.4 基本工具

Skew-T

Hodograph

Radar基础

第二章 对流的触发

2.1 什么是对流

2.2 气块不稳定性

2.3 波动不稳定性

2.4 深湿对流触发

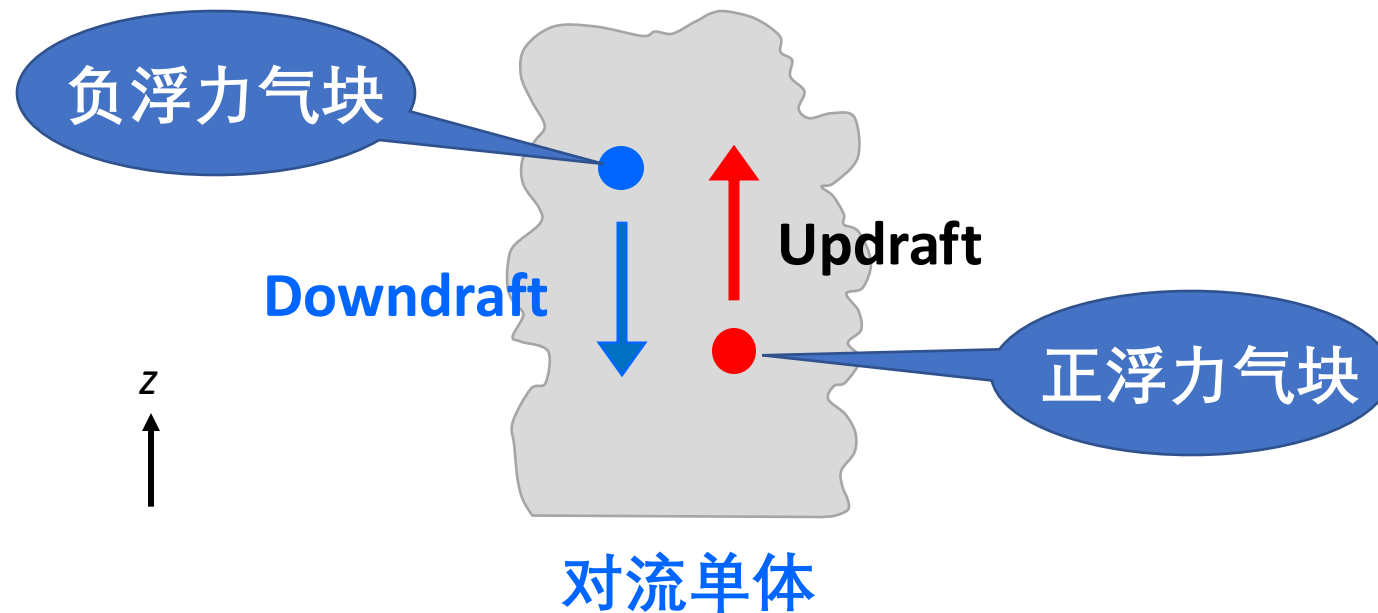
2.5 探空

2.1 什么是对流

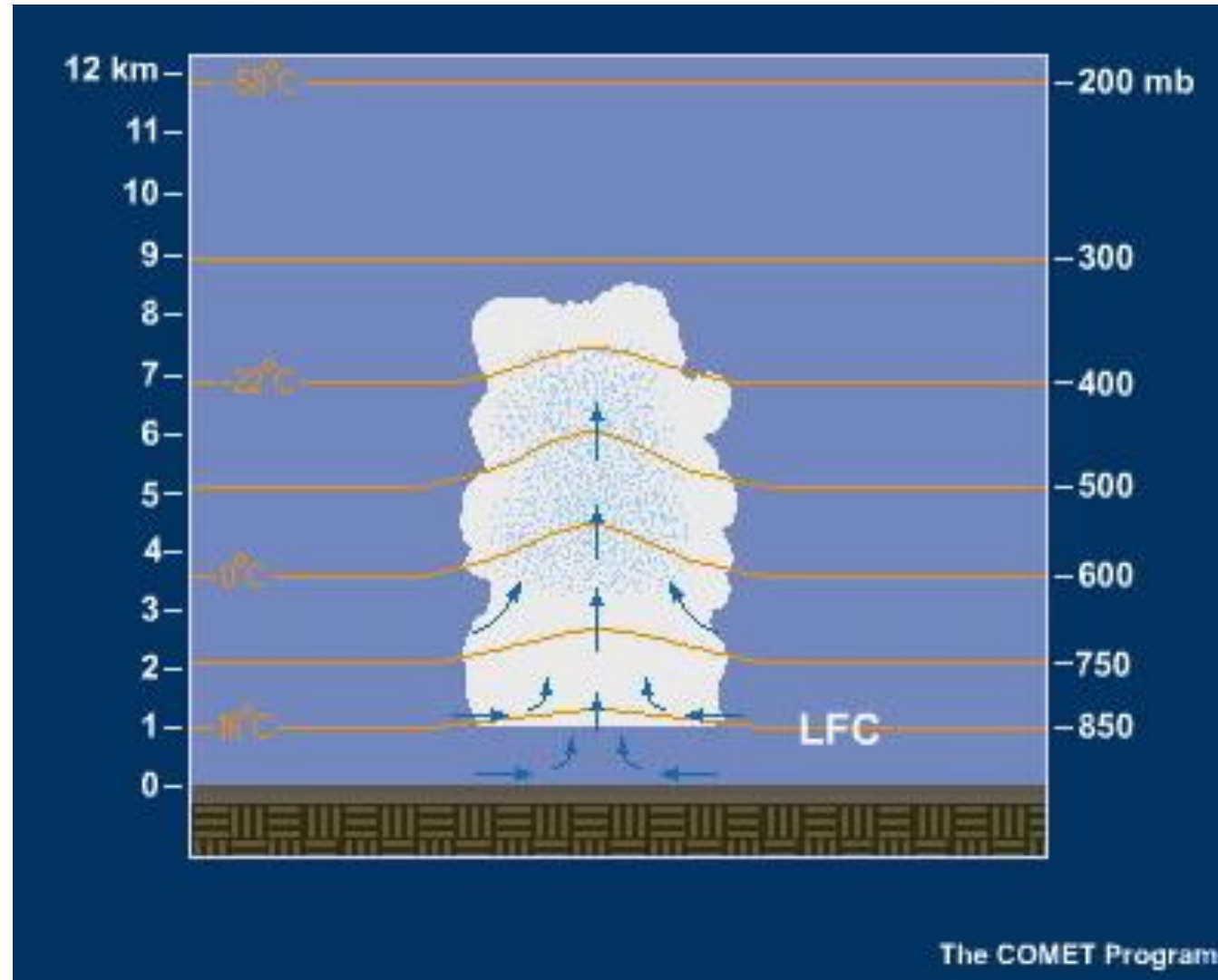
物理定义：指流体运动对某些物理量的传输（比如热量）

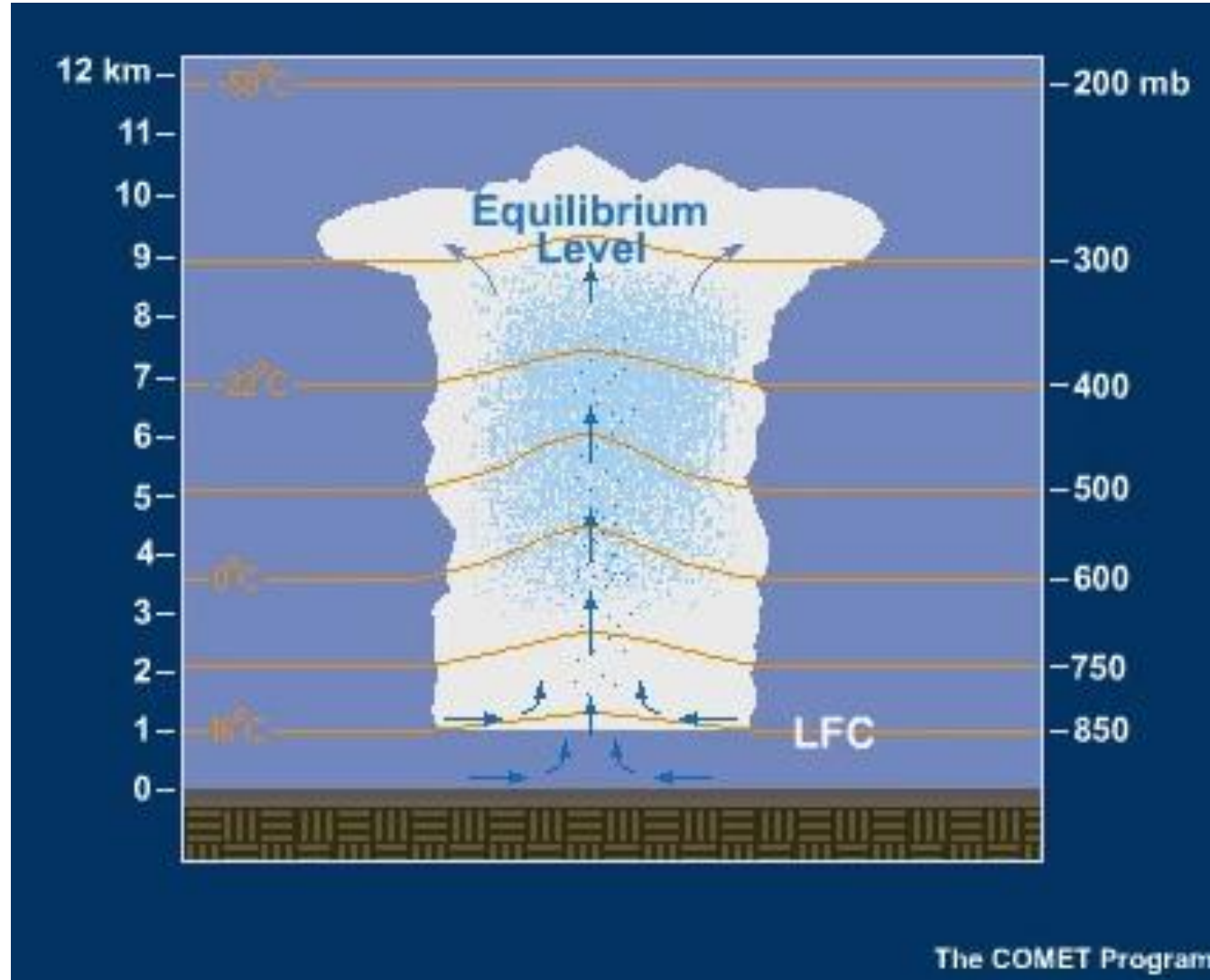
---与传导和辐射不同

气象定义：与浮力有关的气流垂直运动分量对热量的传输

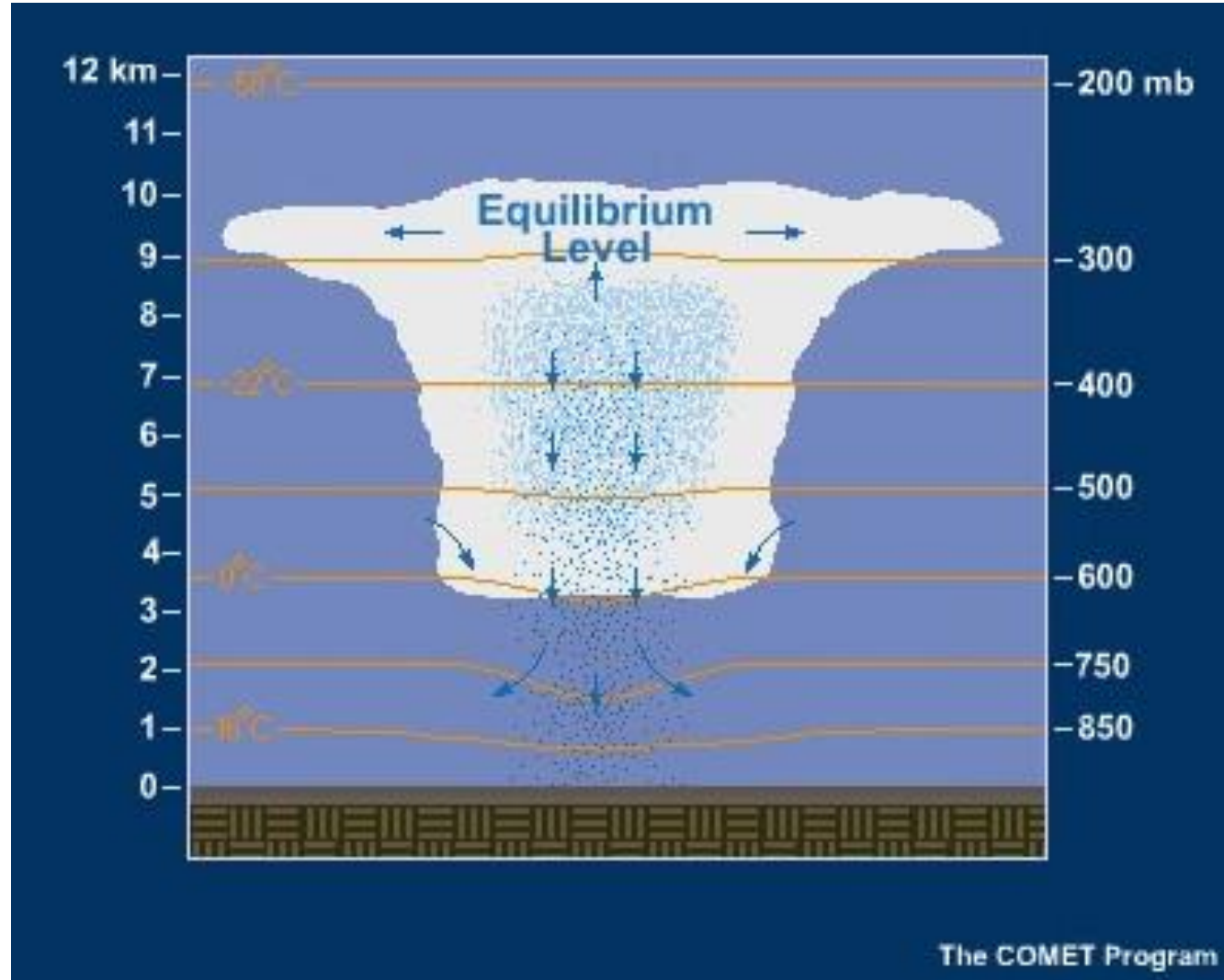


对流发展过程 Stage 1

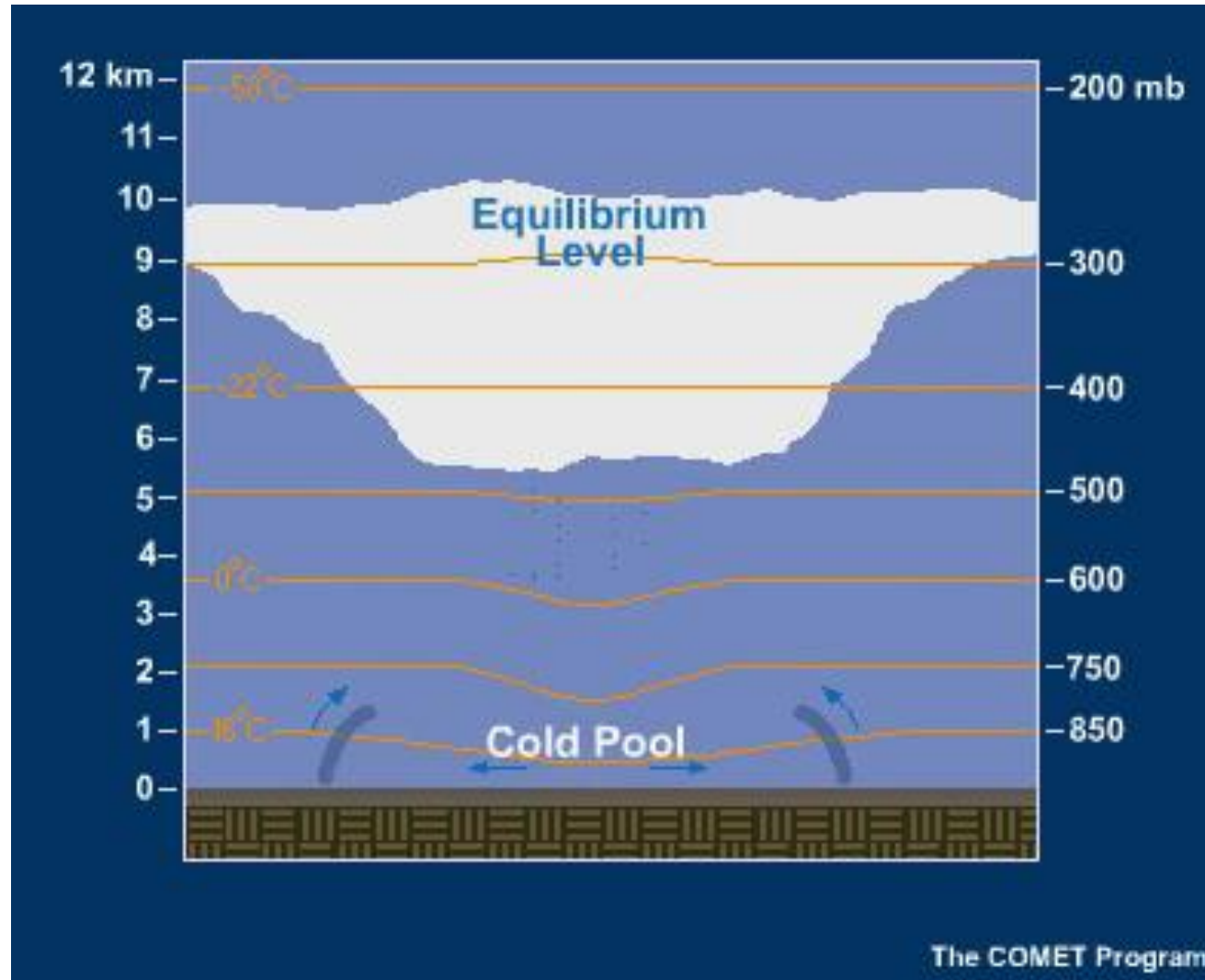




对流发展过程 Stage 3



对流发展过程 Stage 4



Virtual Temperature

In atmospheric thermodynamics, the virtual temperature (T_v) of a moist air parcel is the temperature at which a theoretical dry air parcel would have as total pressure and density equal to the moist parcel of air.

Consider a moist air parcel containing masses m_d and m_v of dry air and water vapor in a given volume V . The density is given by

$$\rho = \frac{m_d + m_v}{V} = \rho_d + \rho_v,$$

where ρ_d and ρ_v are the densities the dry air and water vapor would respectively have when occupying the volume of the air parcel.

Rearranging the standard ideal gas equation with these variables gives

$$e = \rho_v R_v T \text{ and } p_d = \rho_d R_d T.$$

Solving for the densities in each equation and combining with the law of partial pressures yields

$$\rho = \frac{p - e}{R_d T} + \frac{e}{R_v T}.$$

Then, solving for p and using $\epsilon = \frac{R_d}{R_v} = \frac{M_v}{M_d}$ is approximately 0.622 in Earth's atmosphere:

$$p = \rho R_d T_v,$$

where the virtual temperature T_v is

$$T_v = \frac{T}{1 - \frac{e}{p}(1 - \epsilon)}.$$

We now have a non-linear **scalar** for temperature dependent purely on the **unitless** value e/p , allowing for varying amounts of water vapor in an air parcel. This virtual temperature T_v in units of **kelvin** can be used seamlessly in any thermodynamic equation necessitating it.

$$\frac{dw}{dt} = -\frac{1}{\bar{\rho}} \frac{\partial p'}{\partial z} - g \frac{\rho'}{\bar{\rho}} \quad B = -g \frac{\rho'}{\rho_0} \Rightarrow \frac{B}{g} = -\frac{\rho'}{\rho_0}$$

(1) 考虑凝结水的作用

$$p = \rho R_d T_v \quad \text{作变量分解} \quad \frac{p'}{\bar{p}} \approx \frac{\rho'}{\bar{\rho}} + \frac{T_v'}{\bar{T}_v}$$

考虑水凝物，引入广义密度 $\rho_g = \rho(1 + q_h)$

$$\bar{\rho}_g = \bar{\rho} \quad \bar{p} = \bar{\rho} R_d \bar{T}_v \quad \bar{p} = \bar{\rho}_g R_d \bar{T}_v$$

$$\rho = \frac{\rho_g}{(1 + q_h)} \Rightarrow p = \frac{\rho_g}{(1 + q_h)} R_d T_v$$

2.2 浮力



$$p = \frac{\rho_g}{(1 + q_h)} R_d T_v \Rightarrow (1 + q_h)p = \rho_g R_d T_v$$

$$(1 + q_h)\bar{p} \left(1 + \frac{p'}{\bar{p}}\right) = \bar{\rho}_g \left(1 + \frac{\rho_g'}{\bar{\rho}_g}\right) R_d \bar{T}_v \left(1 + \frac{T_v'}{\bar{T}_v}\right)$$

$$q_h + \cancel{\ln \bar{p}} + \frac{p'}{\bar{p}} \approx \cancel{\ln \bar{\rho}_g} + \frac{\rho_g'}{\bar{\rho}_g} + \cancel{\ln R_d} + \cancel{\ln \bar{T}_v} + \frac{T_v'}{\bar{T}_v}$$

$$q_h + \frac{p'}{\bar{p}} \approx \frac{\rho_g'}{\bar{\rho}_g} + \frac{T_v'}{\bar{T}_v}$$

$$\bar{p} = \bar{\rho}_g R_d \bar{T}_v$$

得到考虑水凝物的浮力

$$\frac{B}{g} = -\frac{\rho_g'}{\bar{\rho}_g} \approx \frac{T_v'}{\bar{T}_v} - \frac{p'}{\bar{p}} - q_h$$

2.2 浮力



$$\frac{B}{g} \approx \frac{T_v'}{\bar{T}_v} - \frac{p'}{\bar{p}} - q_h$$

把 $\frac{T_v'}{\bar{T}_v}$ 用位温 θ 表示 $\theta_v = \theta(1 + 0.61q_v)$

$$\theta_v = \theta(1 + 0.61q_v)$$

$$= T \left(\frac{p_0}{p}\right)^{R/c_p} (1 + 0.61q_v)$$

$$= T_v \left(\frac{p_0}{p}\right)^{R/c_p}$$

$$\ln \theta_v = \ln T_v + \frac{R}{c_p} \ln p_0 - \frac{R}{c_p} \ln p$$

$$\cancel{\ln \bar{\theta}_v} + \frac{\theta_v'}{\bar{\theta}_v} \approx \cancel{\ln \bar{T}_v} + \frac{T_v'}{\bar{T}_v} + \frac{R}{c_p} \ln p_0 - \frac{R}{c_p} \ln \bar{p} - \frac{R}{c_p} \frac{p'}{\bar{p}}$$

2.2 浮力



$$\frac{\theta_v'}{\bar{\theta}_v} \approx \frac{T_v'}{\bar{T}_v} - \frac{R p'}{c_p \bar{p}} \quad \text{把} \frac{T_v'}{\bar{T}_v} \text{代入} \quad \frac{B}{g} \approx \frac{T_v'}{\bar{T}_v} - \frac{p'}{\bar{p}} - q_h$$

$$\frac{B}{g} \approx \frac{\theta_v'}{\bar{\theta}_v} + \frac{R p'}{c_p \bar{p}} - \frac{p'}{\bar{p}} - q_h = \frac{\theta_v'}{\bar{\theta}_v} - \frac{c_v p'}{c_p \bar{p}} - q_h$$

$$\theta_v = \theta(1 + 0.61q_v)$$

$$\ln \theta_v = \ln \theta + \ln(1 + 0.61q_v) \approx \ln \theta + 0.61q_v$$

$$\ln (\bar{\theta}_v + \theta_v') \approx \ln (\bar{\theta} + \theta') + 0.61 (\bar{q}_v + q_v')$$

$$\frac{\theta_v'}{\bar{\theta}_v} \approx \frac{\theta'}{\bar{\theta}} + 0.61q_v'$$

$$\ln \bar{\theta}_v \approx \ln \bar{\theta} + 0.61 \bar{q}_v$$

$$\frac{B}{g} \approx \frac{\theta'}{\bar{\theta}} + 0.61q_v' - \frac{c_v p'}{c_p \bar{p}} - q_h$$

升温1K对浮力的贡献相当于：
增加5–6 g/kg 的水汽
减小3–4 hPa的气压
减小 3.3 g/kg的Water loading

(2) 不考虑凝结水、混合、扰动气压的作用(气块法)

$$\frac{B}{g} \approx \frac{\theta'}{\bar{\theta}} = \frac{T'}{\bar{T}} = \frac{T_p - T_e}{T_e}$$
$$B \approx g \frac{T_p - T_e}{T_e}$$

气块法可能高估了浮力

$$\theta = T \left(\frac{p_0}{p}\right)^{R/c_p}$$
$$\frac{\theta'}{\bar{\theta}} = \frac{T'}{\bar{T}} - \frac{R}{c_p} \frac{p'}{\bar{p}}$$

2.2 浮力



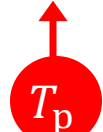
浮力可解释为由于空气块和周围环境温差（密度差）而施加在空气块上的向上或向下的力，是对流风暴的关键因子。


$$B \equiv g \frac{T_p - T_e}{T_e} \quad \text{单位: } \text{m s}^{-2}$$

g : 重力加速度

T_p : 气块的温度

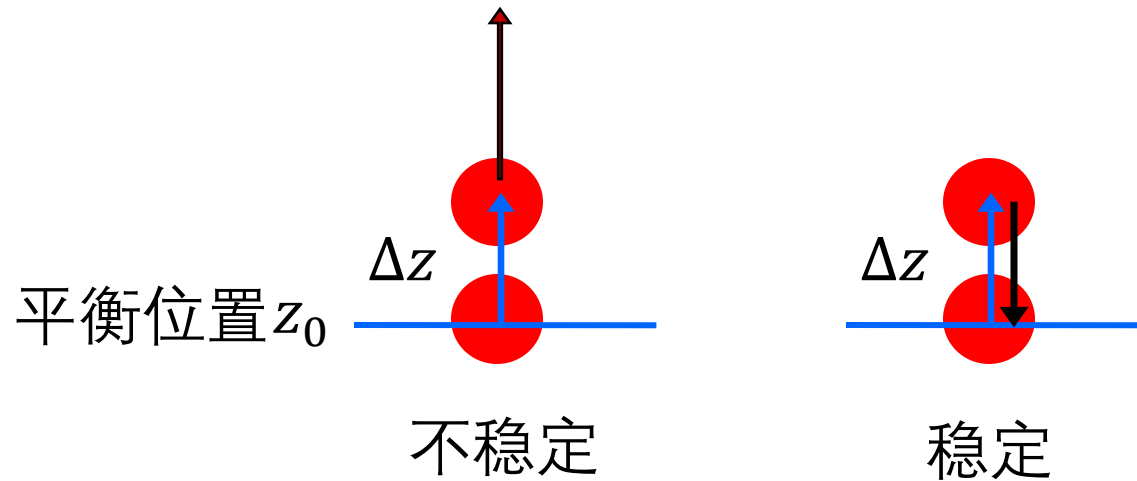
T_e : 环境的温度（探空温度廓线）

B 可正可负 如果 $T_p > T_e$, $B > 0$,  T_e 气块向上加速

如果 $T_p < T_e$, $B < 0$,  T_e 气块向下加速

2.3 静力稳定度分析

环境的静力稳定度：由垂直方向偏离平衡位置的空气块受到的浮力决定。



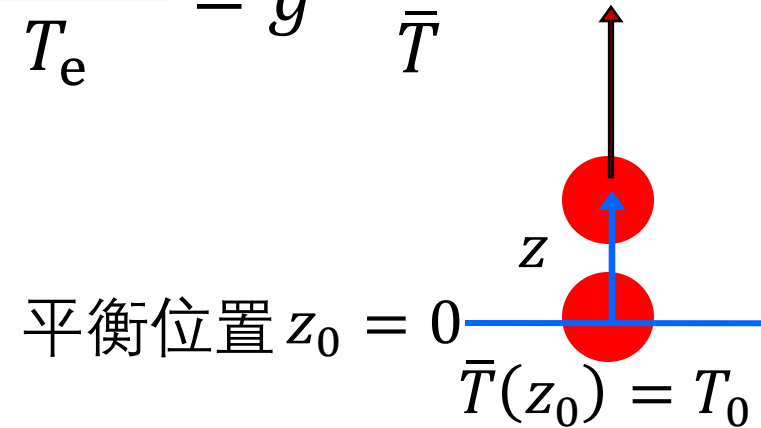
静力稳定度的判断：求解 Δz 随时间的变化

2.3 静力稳定度分析

垂直运动方程（忽略气压梯度力、摩擦力、科氏力）

$$\frac{dw}{dt} = B \quad w = \frac{dz}{dt} \quad B \equiv g \frac{T_p - T_e}{T_e} = g \frac{T - \bar{T}}{\bar{T}}$$

$$\frac{d^2z}{dt^2} = g \frac{T - \bar{T}}{\bar{T}}$$



环境垂直减温率 $\gamma = -\frac{\partial \bar{T}}{\partial z}$ 气块垂直减温率 $\Gamma_p = -\frac{\partial T}{\partial z}$

干绝热减温率 Γ_d , $1^\circ\text{C}/100\text{m}$, $10^\circ\text{C}/1\text{km}$, $\sim \frac{g}{c_p} = 9.8^\circ\text{C}/1\text{km}$

湿绝热减温率 Γ_m , $3-7^\circ\text{C}/1\text{km}$, (与 q_v 有关)

2.3 静力稳定度分析

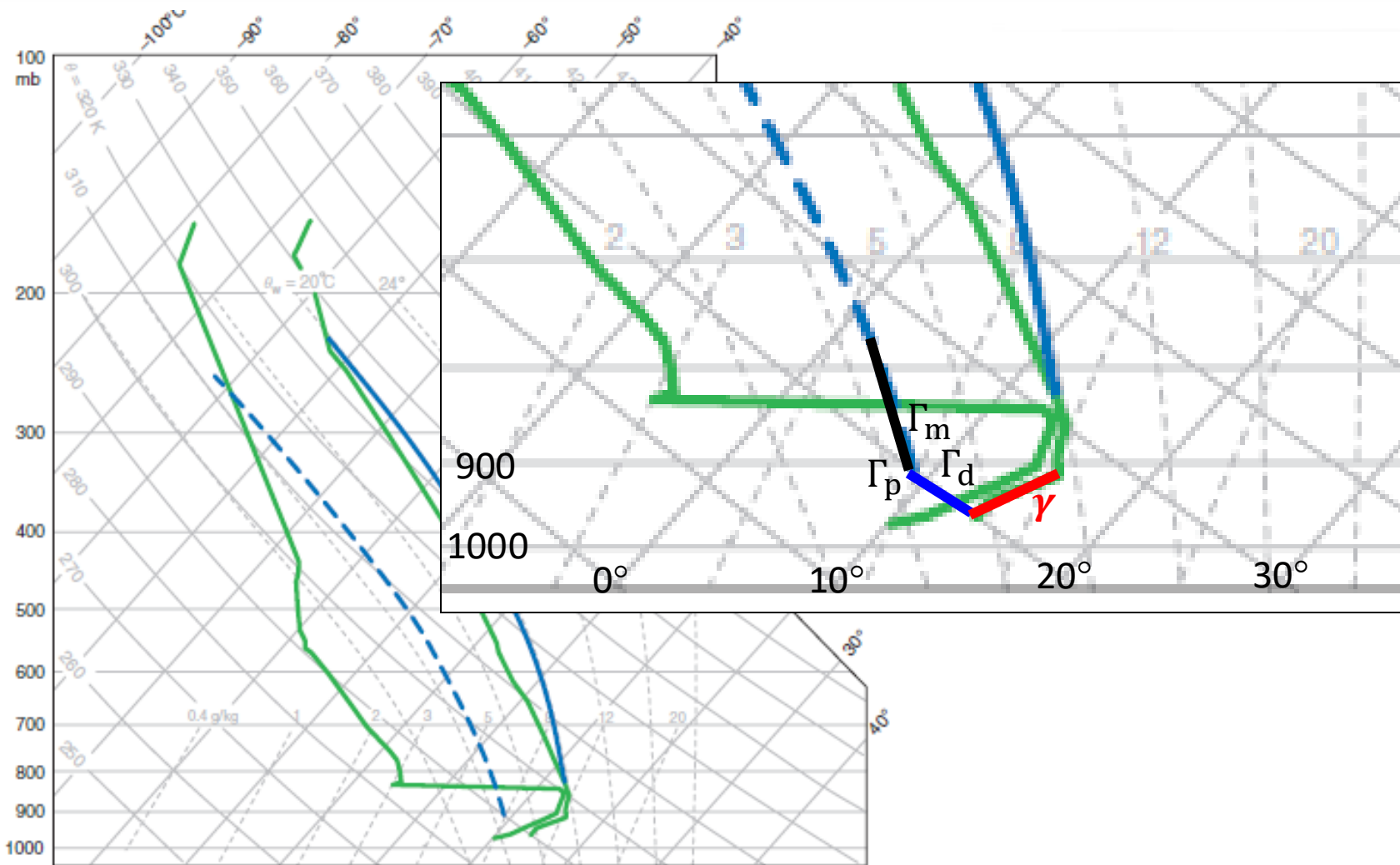


Figure 7.22 Example of a sounding containing elevated CAPE but no surface-based CAPE. A parcel of air lifted from the surface follows the dashed blue trajectory, whereas an air parcel lifted from the top of the stable boundary layer follows the solid blue trajectory.

2.3 静力稳定度分析

$$\bar{T} = T_0 - \gamma z \quad T = T_0 - \Gamma_p z$$

$$\frac{d^2 z}{dt^2} = g \frac{T - \bar{T}}{\bar{T}} = g \frac{T_0 - \Gamma_p z - T_0 + \gamma z}{T_0 - \gamma z} = -g \frac{\Gamma_p - \gamma}{T_0 - \gamma z} z$$

如果 Δz 很小, $T_0 \gg \gamma z$, 可以得到

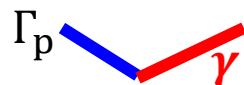
$$\frac{d^2 z}{dt^2} + \frac{g}{T_0} (\Gamma_p - \gamma) z = 0$$

$$z(t) = c_1 e^{i \left[\frac{g}{T_0} (\Gamma_p - \gamma) \right]^{1/2} t} + c_2 e^{-i \left[\frac{g}{T_0} (\Gamma_p - \gamma) \right]^{1/2} t}$$

c_1, c_2 由气块初始扰动的大小和方向决定

2.3 静力稳定度分析

(1) $\gamma < \Gamma_p$



$z(t)$ 的实部可写为 $z(t) = c \cos \left\{ \left[\frac{g}{T_0} (\Gamma_p - \gamma) \right]^{1/2} t \right\}$

因而环境是静力稳定的。

非饱和情况下，振动频率为 $\left[\frac{g}{T_0} (\Gamma_d - \gamma) \right]^{1/2}$ Brunt-Vaisala频率

推导该频率的位温形式

热力学第一定律 $dq = c_p dT - \alpha dp$

$$dq = c_p dT - \frac{RT}{p} dp \quad \frac{dq}{T} = c_p \frac{dT}{T} - R \frac{dp}{p} \quad \textcircled{1}$$

2.3 静力稳定度分析

$$\theta = T \left(\frac{1000}{p} \right)^{R/c_p} \quad \text{两边取对数: } \ln \theta = \ln T + c - \frac{R}{c_p} \ln p$$

$$\text{两边求微分: } \frac{d\theta}{\theta} = \frac{dT}{T} - \frac{R}{c_p} \frac{dp}{p}$$

$$c_p \frac{d\theta}{\theta} = c_p \frac{dT}{T} - R \frac{dp}{p} \quad \textcircled{2}$$

$$\textcircled{1} \text{ 代入 } \textcircled{2}: \quad c_p \frac{d\theta}{\theta} = \frac{dq}{T} \quad \textcircled{3}$$

$$\frac{dq}{T} = c_p \frac{dT}{T} - R \frac{dp}{p}$$

$$\frac{dp}{dz} = -\frac{1}{\alpha} g \quad \Rightarrow \quad \alpha dp = -g dz$$

$$dq = c_p dT - \alpha dp = c_p dT + g dz \quad \text{把 } dq \text{ 代入 } \textcircled{3}$$

2.3 静力稳定度分析

$$c_p \frac{d\theta}{\theta} = \frac{1}{T} (c_p dT + g dz) \quad \text{两边除以 } c_p dz:$$

$$\frac{1}{\theta} \frac{d\theta}{dz} = \frac{1}{T} \left(\frac{dT}{dz} + \frac{g}{c_p} \right) \quad \text{对于平衡位置处的小扰动, 可近似为:}$$

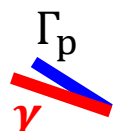
$$\frac{1}{\theta_0} \frac{\Delta\bar{\theta}}{\Delta z} = \frac{1}{T_0} \left(\frac{\Delta T}{\Delta z} + \Gamma_d \right) \Rightarrow \frac{1}{\theta_0} \frac{\partial \bar{\theta}}{\partial z} = \frac{1}{T_0} (\Gamma_d - \gamma)$$

$$\text{因而 } \left[\frac{g}{T_0} (\Gamma_p - \gamma) \right]^{1/2} = \left[\frac{g}{\theta_0} \frac{\partial \bar{\theta}}{\partial z} \right]^{1/2} = N$$

$$\gamma < \Gamma_p \Rightarrow \frac{\partial \bar{\theta}}{\partial z} > 0$$

$$\text{饱和情况下, 振动频率为 } N_m = \left[\frac{g}{\theta_e} \frac{\Gamma_m}{\Gamma_d} \frac{\partial \bar{\theta}_e^*}{\partial z} \right]^{1/2}$$

2.3 静力稳定度分析

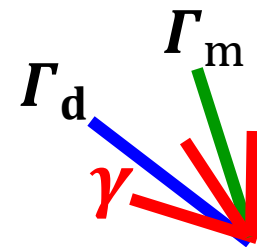
(2) $\gamma > \Gamma_p$  $z(t) = c_1 e^{i \left[\frac{g}{T_0} (\Gamma_p - \gamma) \right]^{1/2} t} + c_2 e^{-i \left[\frac{g}{T_0} (\Gamma_p - \gamma) \right]^{1/2} t}$

$$z(t) \propto c e^{\left[\frac{g}{T_0} (\gamma - \Gamma_p) \right]^{1/2} t}$$

Δz 随 t 指数增大，因而环境是静力不稳定的。

静力
稳定
度判
据小
结

- $\gamma > \Gamma_d$ 绝对不稳定 $\frac{\partial \bar{\theta}}{\partial z} < 0$
- $\Gamma_m < \gamma < \Gamma_d$ 条件性不稳定 $\frac{\partial \bar{\theta}_e^*}{\partial z} < 0$
- $\gamma < \Gamma_m$ 绝对稳定 $\frac{\partial \bar{\theta}_e^*}{\partial z} > 0$
- $\gamma = \Gamma_d$ 中性 (相对于未饱和气块扰动) $\frac{\partial \bar{\theta}}{\partial z} = 0$
- $\gamma = \Gamma_m$ 中性 (相对于饱和气块扰动) $\frac{\partial \bar{\theta}_e^*}{\partial z} = 0$



2.4 对流有效位能 CAPE

(1) 定义：气块法中上升气块所获得的最大能量。

把浮力从自由对流高度（首次 $T_p > T_e$ ）积分到平衡高度（最后一次 $T_p < T_e$ ）所得的积分结果称为**CAPE**（Convective Available Potential Energy）。

$$\text{CAPE} \equiv \int_{z=\text{LFC}}^{z=\text{EL}} B dz$$

$$= g \int_{z=\text{LFC}}^{z=\text{EL}} \frac{T_p(z) - T_e(z)}{T_e(z)} dz$$

$$B \approx g \frac{T_p - T_e}{T_e}$$

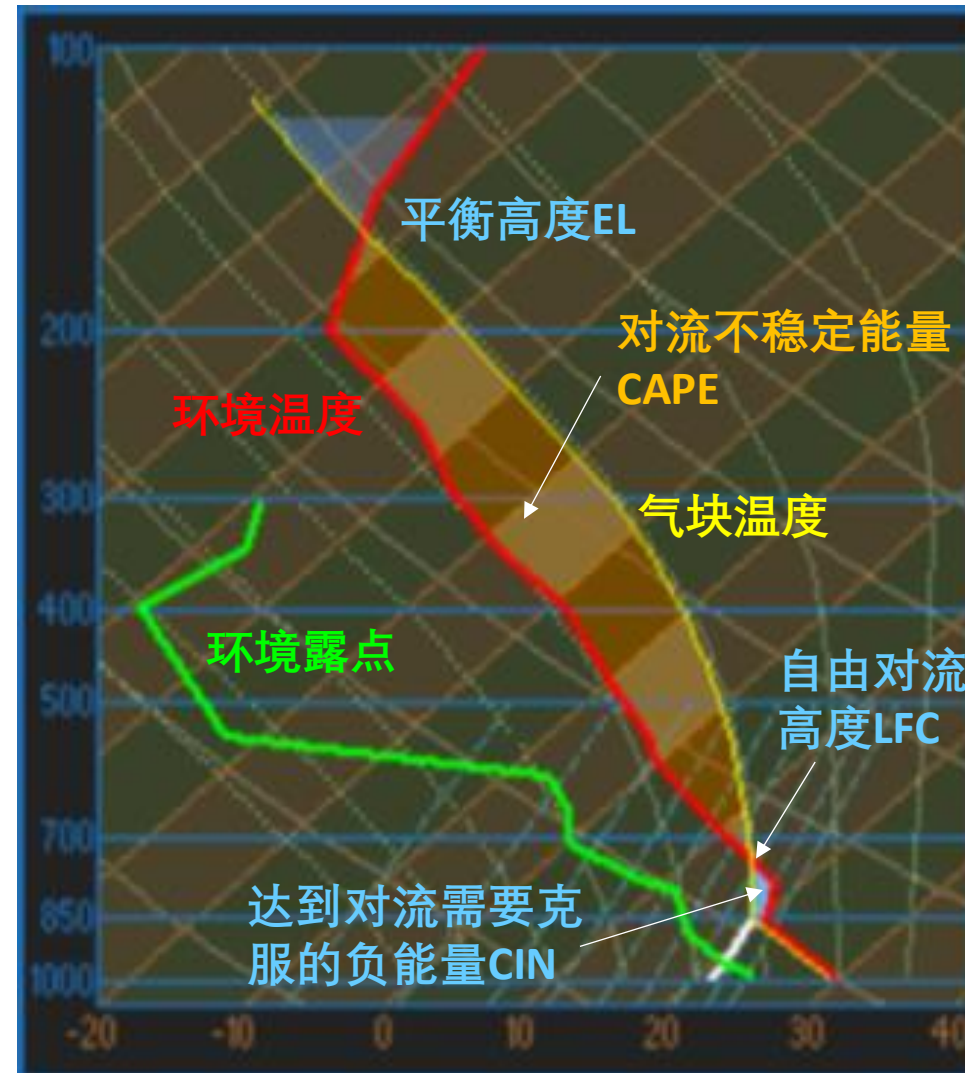
①

正负面积之和

单位：J/kg 或 m^2s^{-2}

2.4 对流有效位能 CAPE

- CAPE是强对流天气的主要能源之一，是深湿对流的必要条件，反映的是条件性不稳定。
- CAPE在Skew-T图上表示为 T_e 和湿绝热线之间的面积夹在LFC和EL之间的部分。



(MetED/NCAR)

2.4 对流有效位能 CAPE

(2) CAPE和对流上升气流 (Updraft)

考虑浮力引起的垂直加速度

$$\frac{dw}{dt} \approx g \frac{T_p - T_e}{T_e} = B \quad \textcircled{2}$$

$$w \frac{dw}{dt} = Bw$$

$$\frac{1}{2} \frac{dw^2}{dt} = B \frac{dz}{dt}$$

$$dw^2 = 2Bdz$$

从LFC到EL对上式积分

$$\int_{w_{LFC}}^{w_{EL}} dw^2 = \int_{z=LFC}^{z=EL} 2Bdz$$

2.4 对流有效位能 CAPE

$$\int_{w_{LFC}=0}^{w_{EL}=w_{max}} dw^2 = \int_{z=LFC}^{z=EL} 2Bdz$$

$$CAPE \equiv \int_{z=LFC}^{z=EL} Bdz$$

$$w_{max}^2 = 2CAPE \quad w_{max} = \sqrt{2CAPE}$$

因此，利用气块法，我们可以计算具有一定CAPE的对流云所能达到的最大上升速度

(a) Role of thumb

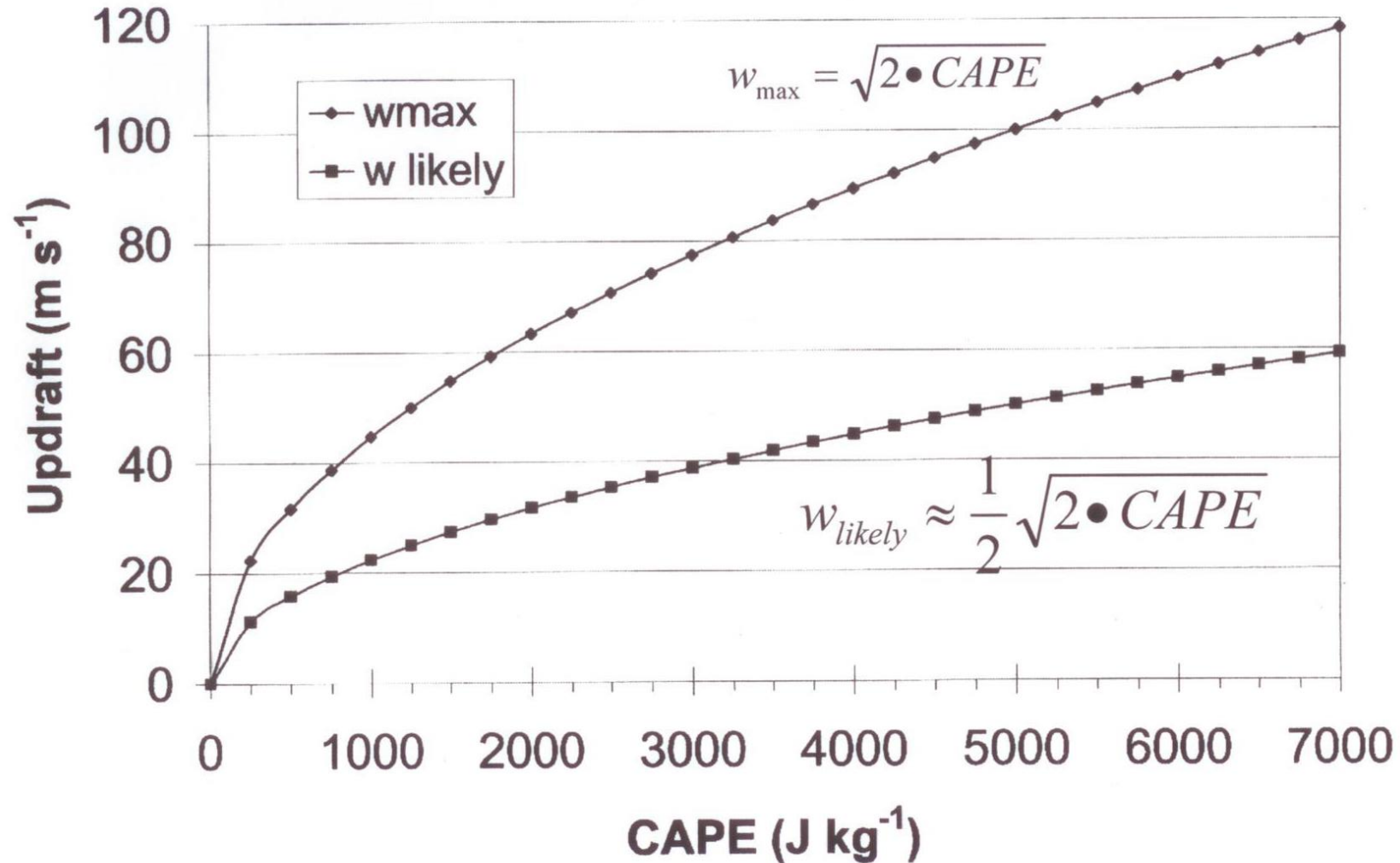
对普通的对流单体，CAPE的典型值为1000J/kg.

$$w_{max} = \sqrt{2000\text{m}^2\text{s}^{-2}} = 45\text{m s}^{-1}$$

气块法忽略了气块与外界的动量、热量、和水汽的混合，因而往往高估对流的上升速度，一般观测为10-20m s⁻¹。

2.4 对流有效位能 CAPE

Updraft estimate using parcel theory



2.4 对流有效位能 CAPE

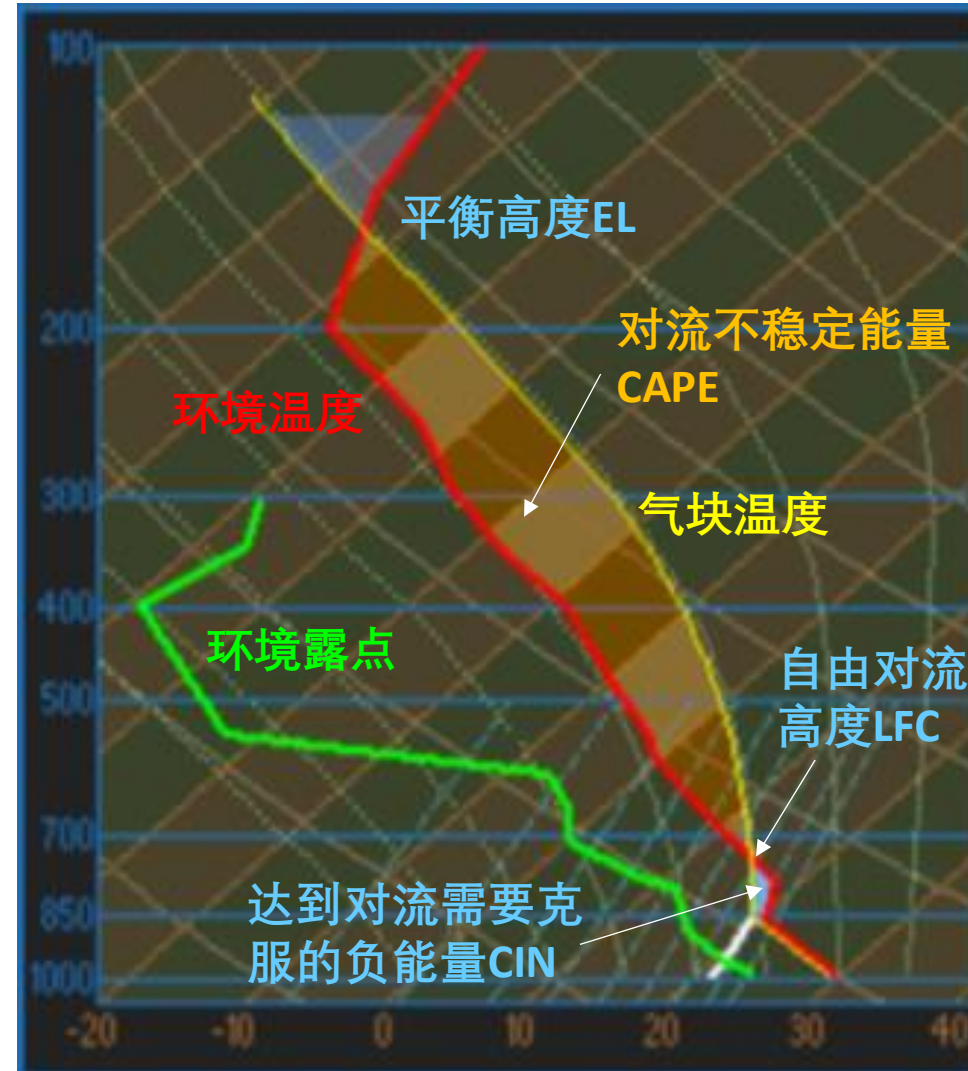
影响CAPE的因素:

环境减温率

绝热减温率

抬升气块选择

LFC和EL



2.4 对流有效位能 CAPE

影响CAPE的因素：环境减温率、绝热减温率、抬升气块选择、LFC和EL

气块法忽略了

1) 液态水 $q_h > 0$, 减小浮力

2) 扰动气压 $p' > 0$, 浮力减小

扰动气压梯度力向下, 减小上升速度

$$\frac{B}{g} \approx \frac{\theta'}{\bar{\theta}} + 0.61q_v' - \frac{c_v p'}{c_p \bar{p}} - q_h$$

3) 夹卷效应 (环境向气块内部的干空气混合)

其影响与Updraft的宽度成反比

超级单体或较大的有组织的风暴更易出现接近于气块法得到的最大上升速度 (较少的卷入)

$T' < 0$, 冷却, 绝热曲线往左偏, CAPE变小

$q_v' < 0$, 减小浮力

夹卷效应对CAPE的影响

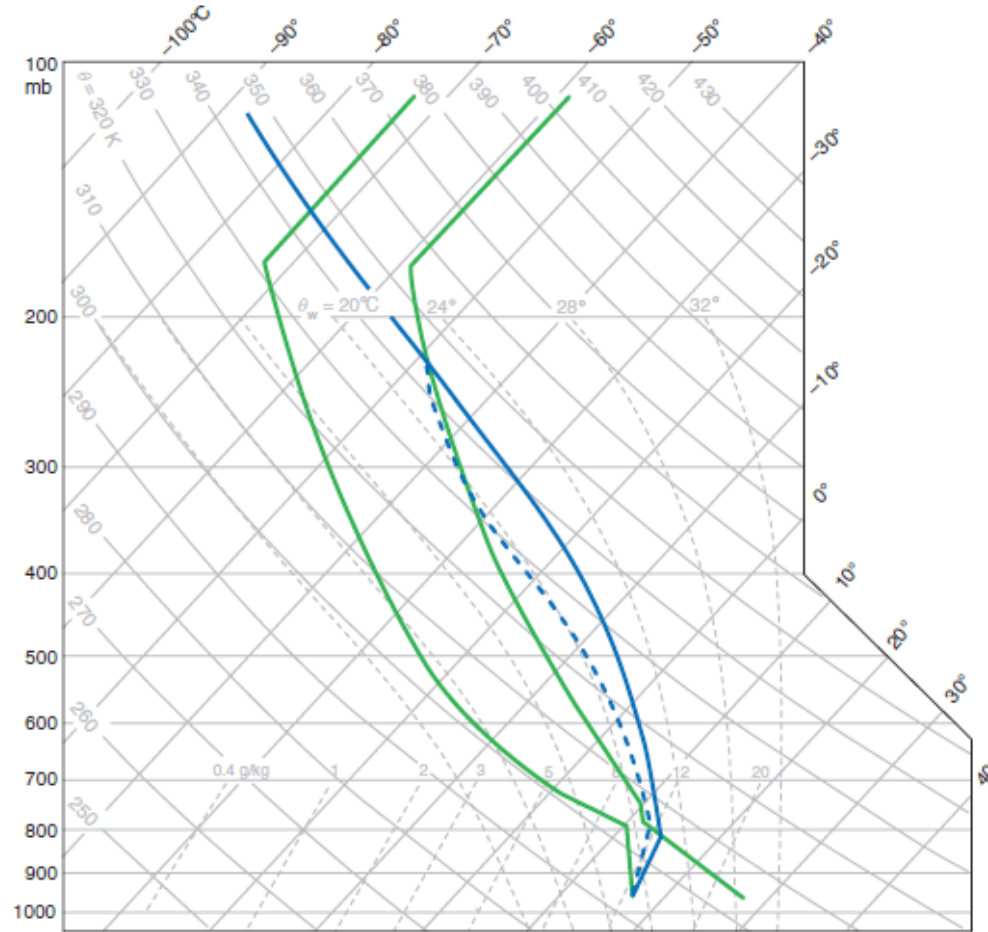


Figure 3.2 A possible parcel process curve (dashed) that might be followed by an updraft parcel on a skew T -log p diagram as a result of the entrainment of environmental air. A parcel process curve (solid) followed by an updraft parcel that ascends undiluted is also shown. Note the implied differences in cloud base (there has been some entrainment below the cloud base, in addition to entrainment over the cloud depth), cloud top, and the realized CAPE.

夹卷效应对CAPE的影响

(CAPE: 红色等值线)

没考虑干空气混合

考虑了干空气混合

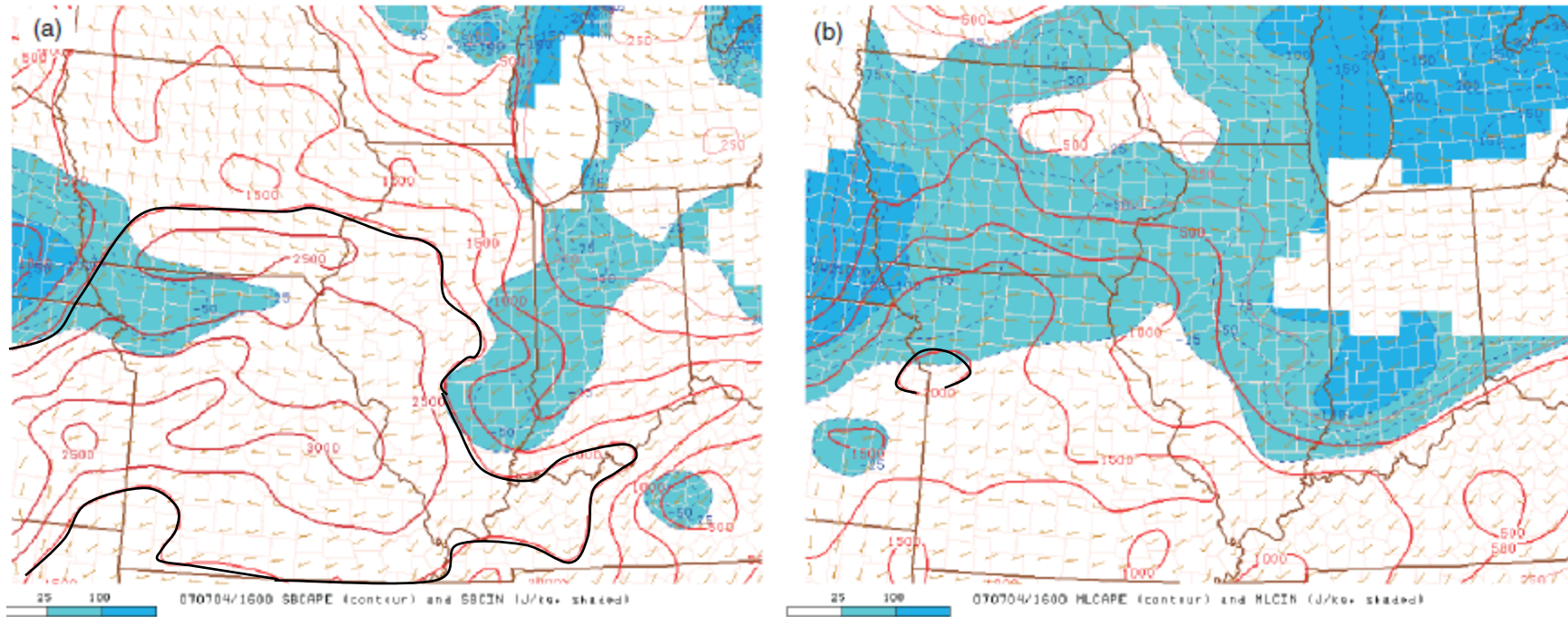


Figure 7.18 Comparison of CAPE (red contours; J kg^{-1}) and CIN values (blue shading; J kg^{-1}) computed by lifting (a) a parcel from the surface, assuming no mixing, and (b) a parcel having the mean potential temperature and water vapor mixing ratio of the lowest 100 mb, which crudely attempts to account for mixing that occurs en route to the LFC. CAPE (CIN) values are typically smaller (larger) when a parcel is lifted having the mean properties of the lowest 100 mb (or some layer of roughly similar depth), as is the case above, except perhaps at night or on the cold side of a front, where a shallow layer of relatively cool air might be found near the surface. (Courtesy of the Storm Prediction Center.)

2.4 对流有效位能 CAPE

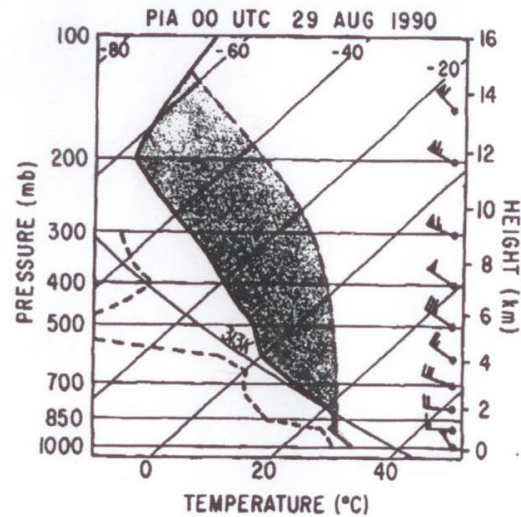
(2) 典型CAPE值

对流强度	CAPE (J/kg)	气块法预测的 w_{max} ($m s^{-1}$)	可能的实际 w ($m s^{-1}$)
弱-中等强度	< 1000	< 45	< 22.5
中-强	1000-3000	45-77	22.5-38.5
强-很强	3000-8000	77-126	38.5-63

CAPE极端个例

Extreme CAPE and an F5 tornadic supercell Plainfield, IL August 28, 1990 (Seimon, 1993, BAMS)

CAPE \approx
8000 J kg⁻¹



Bulletin American Meteorological Society

FIG. 4. Sounding in skew T-log p format from Peoria, Illinois (PIA), at 0000 UTC 29 August 1990. Temperature (solid) and dewpoint (dashed) are shown along with a representative dry adiabatic (313 K). Estimated parcel trajectory from the lifted condensation level is indicated, along with the region of positive potential buoyant energy (shading). Winds in m s⁻¹ with pennant, barb, and half barb denoting 25, 5, and 2.5 m s⁻¹, respectively.

Skew-T Log P diagram
with CAPE highlighted

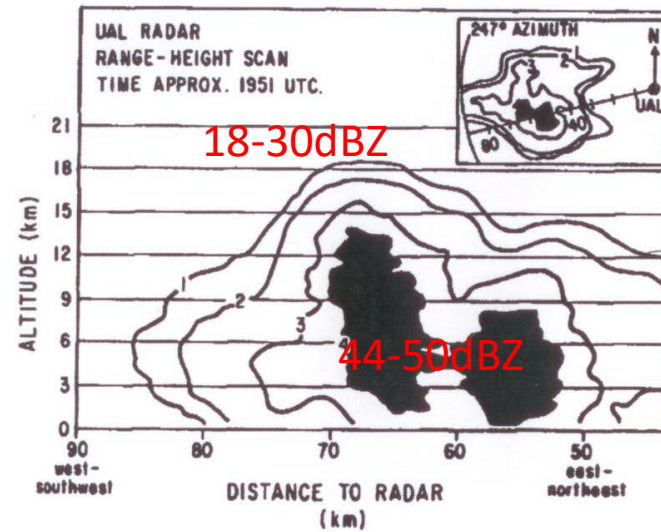


FIG. 10. Vertical radar cross section of the Plainfield storm at 1951 UTC (time estimated) from a range-height indicator (RHI) scan performed by the United Airlines (UAL) radar at Elk Grove, Illinois. Corresponding plan-position indicator (PPI) scan of the storm at 1° elevation angle is provided in inset window, with RHI beam azimuth (247°) depicted along with 10-km range markers. VIP levels 1-4 are indicated, with light shading denoting regions of VIP 3 and dark shading VIP 4, where VIP 4 indicates reflectivity \geq 45 dBZ.

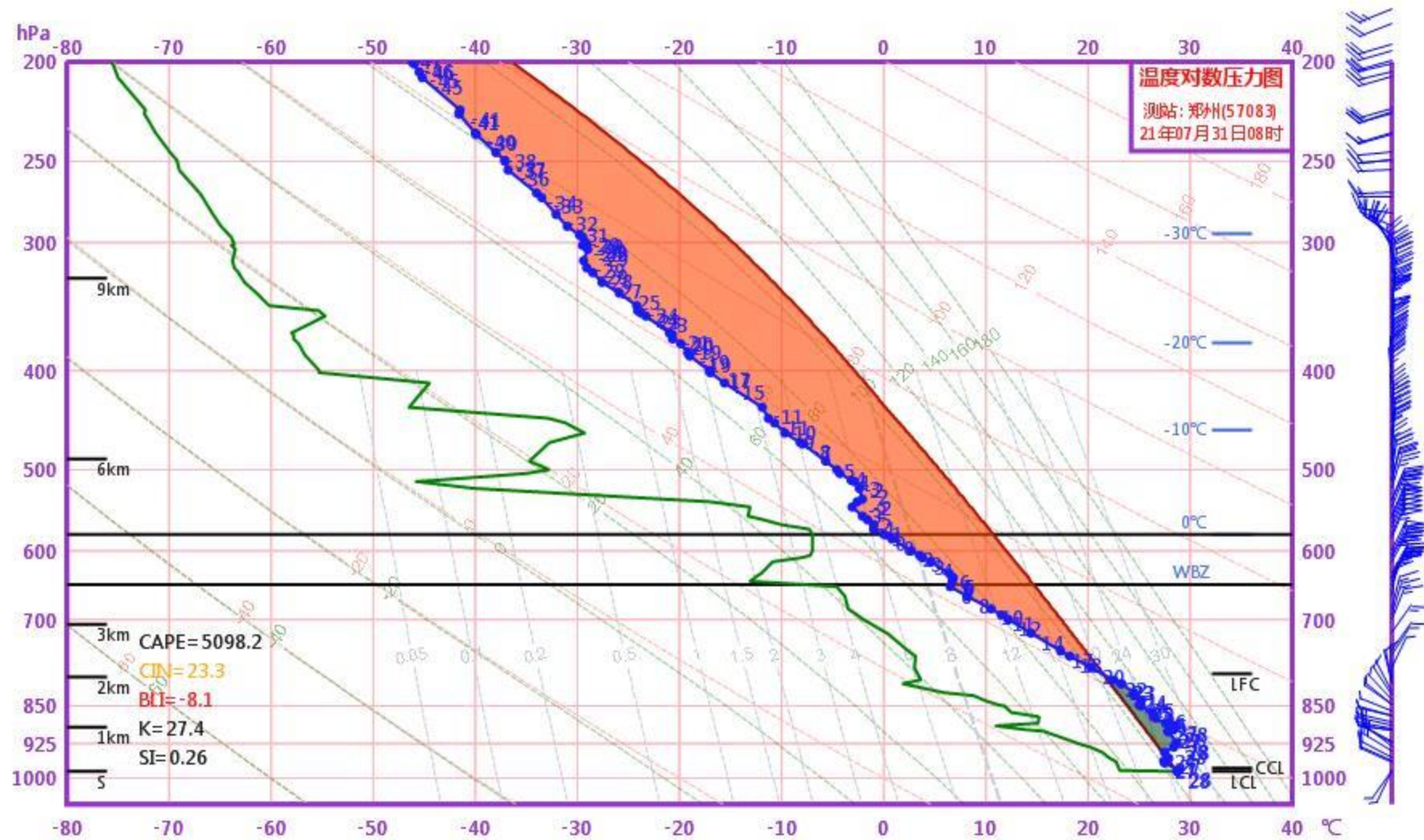
Vertical cross-section of storm
structure (inset: horizontal structure)

闪电

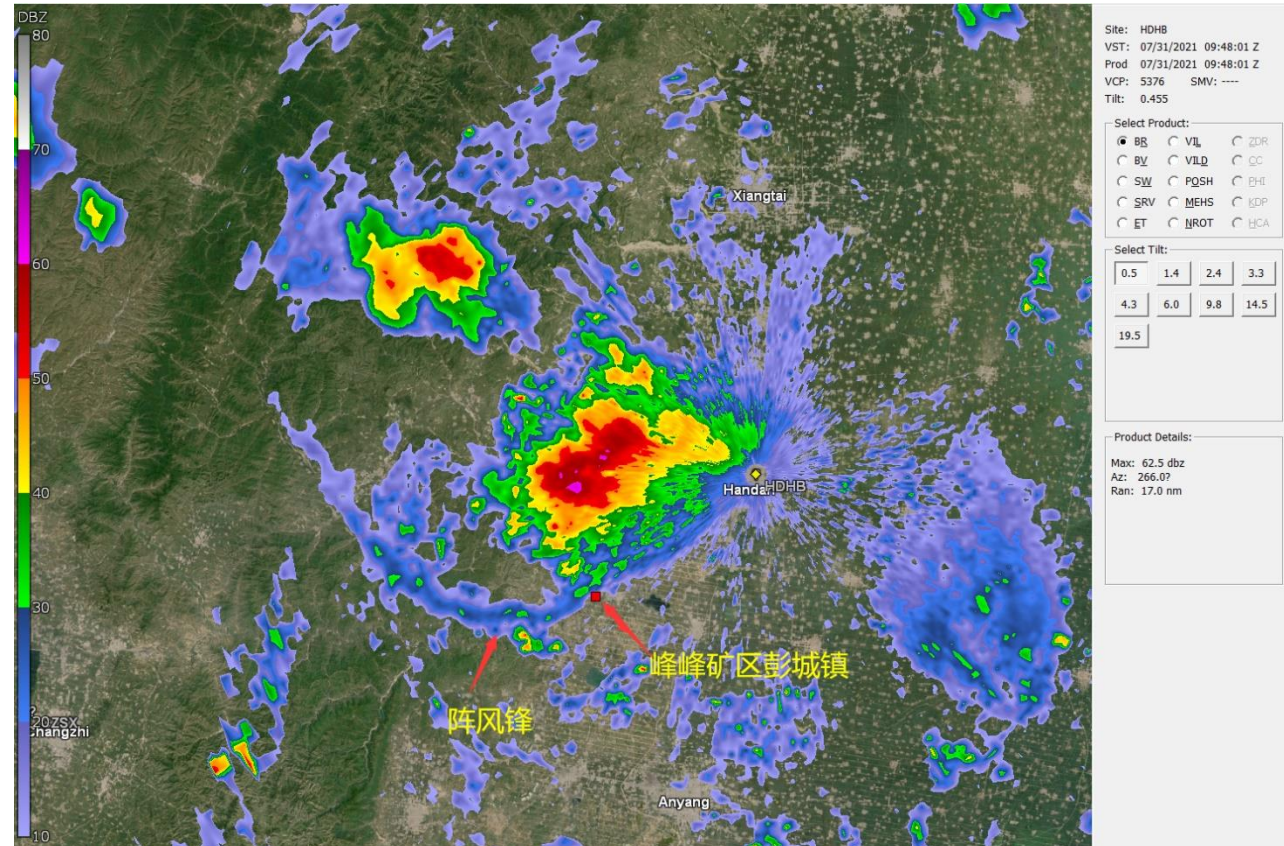
冰雹
龙卷

$W_{max} = 126$
 $m s^{-1}$, 即使一半也还有
 $63 m s^{-1}$

极端CAPE举例：2021.7.31邯鄲大风




极端CAPE举例：2021.7.31邯鄲大风



极端CAPE举例：2021.7.31邯鄲大风



On the Physics of High CAPE

KERRY EMANUEL ^a

^a *Lorenz Center, Massachusetts Institute of Technology, Cambridge, Massachusetts*

(Manuscript received 1 April 2023, in final form 5 July 2023, accepted 5 September 2023)

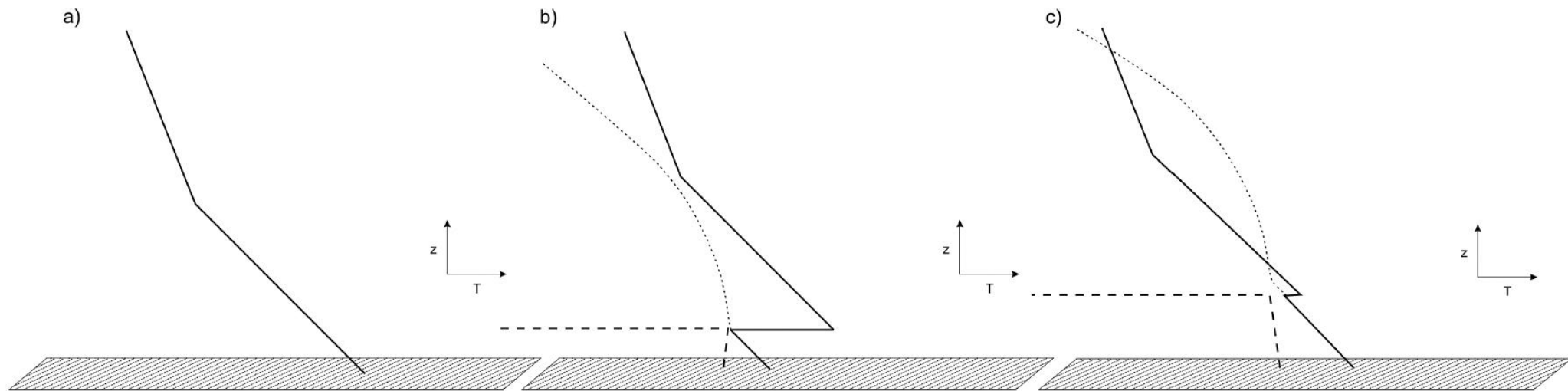


FIG. 1. Three stages in the diurnal evolution of CAPE. (a) A desert-modified air mass with little moisture and a deep dry adiabatic boundary layer is advected over a moist soil. (b) Advection of cool, moist air from a different region and/or wind-driven boundary layer turbulence creates a moist but cool new shallow boundary layer just saturated at its top. Dewpoint is shown by dashed lines, and the temperature of a parcel lifted adiabatically is shown by the dotted curve. (c) Surface heating by solar radiation causes the now-convective boundary layer to deepen and moisten, though the moistening is at least partially offset by entrainment of dry air from above the boundary layer. CIN decreases and CAPE increases, with the proportion depending on surface moisture availability.

Atmospheric Model

$$\rho h \frac{dD}{dt} = F_s + \rho w_e (D_0 - D),$$

$$\rho h \frac{dM}{dt} = F_s + F_L + \rho w_e (D_0 - M),$$

$$\frac{\partial T_s}{\partial t} = C_T (F_{\text{net}} - F_s - F_L) - \frac{\pi}{t_0} (T_s - T_2),$$

$$\frac{\partial T_2}{\partial t} = \frac{1}{2t_0} (T_s - T_2),$$

Soil and Vegetation Model

$$\frac{\partial q_g}{\partial t} = \frac{-C_1}{\rho_w d_1} E_{\text{soil}} - \frac{C_2}{2t_0} (q_g - q_{\text{geq}}),$$

$$\frac{\partial q_2}{\partial t} = \frac{-1}{\rho_w d_2} (E_{\text{soil}} + E_{\text{veg}}),$$

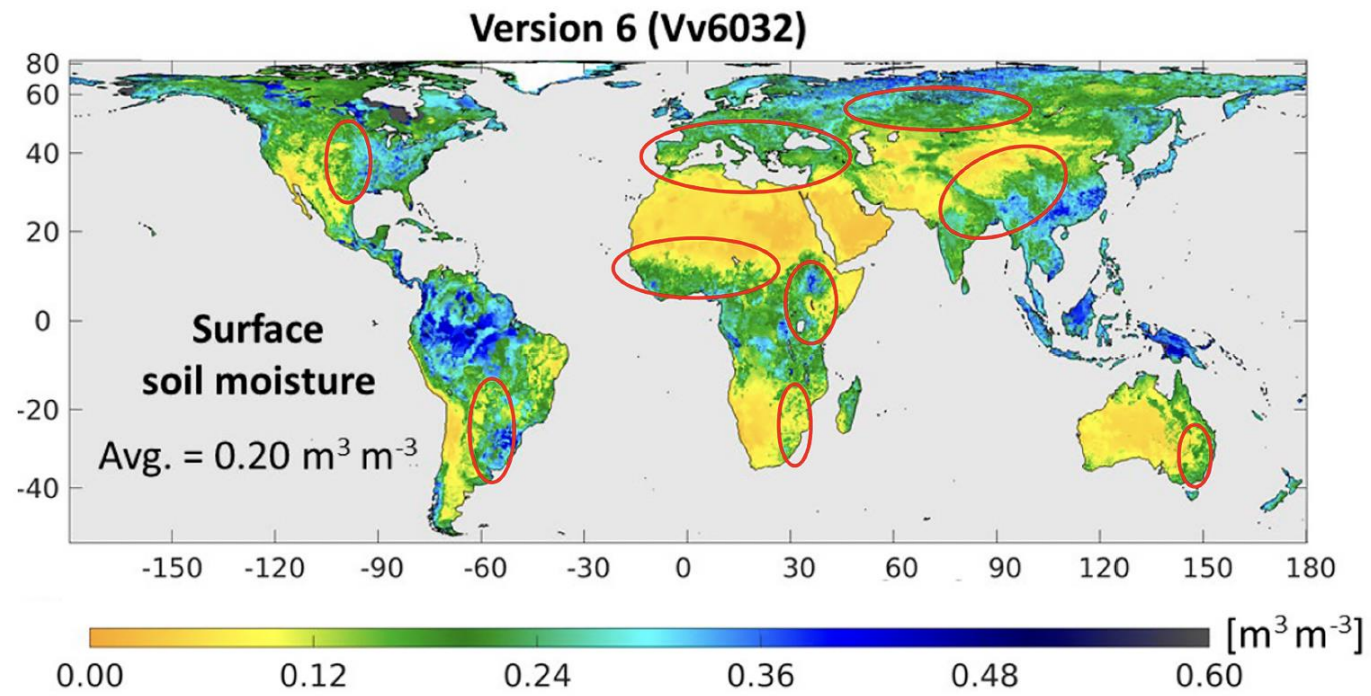


FIG. 11. Surface soil moisture measured by the Soil Moisture Active Passive (SMAP) project averaged over the period April 2015–March 2021 (Reichle et al. 2022). This is based on level 4 SMAP data. The red ellipses show areas of moist soils downwind from dry terrain, as described in the text.

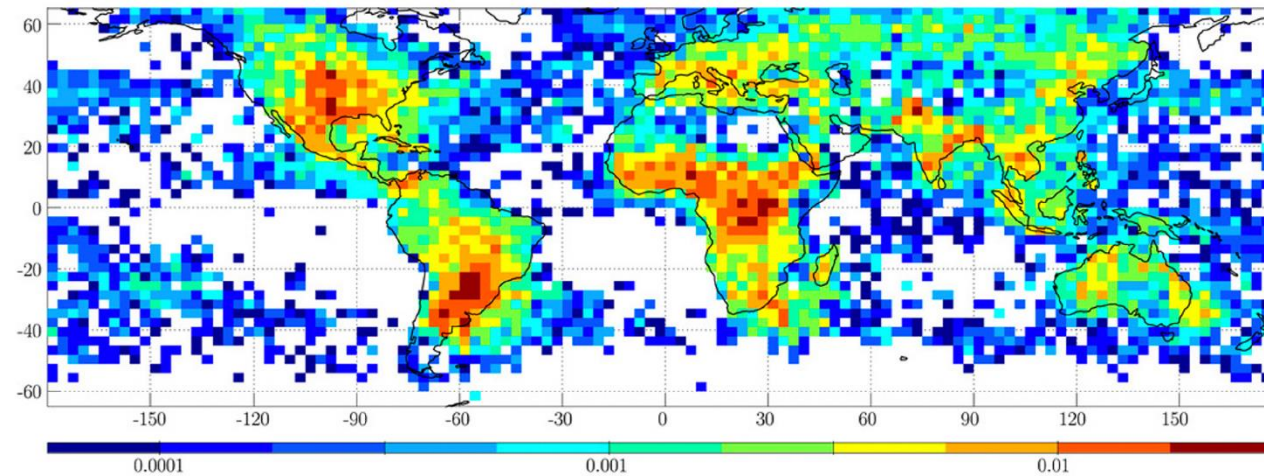


FIG. 12. Percentage of Dual-Frequency Precipitation Radar soundings from GPM satellites that contain hail, based on the mean Ku-band reflectivity in the mixed-phase layer. From Mroz et al. (2017).